ELSEVIER

Marine Geology 193 (2003) 49–59

MARINE GEOLOGY
INTERNATIONAL JOURNAL OF MARINE GEOLOGY, GEOCHEMISTRY AND GEOPHYSICS

www.elsevier.com/locate/margeo

# Asymmetric sedimentation on young ocean floor at the East Pacific Rise, 15°S

Jan Hauschild *, Ingo Grevemeyer, Norbert Kaul, Heinrich Villinger

*Department of Earth Sciences, University of Bremen, 28334 Bremen, Germany*

Received 21 December 2001; accepted 24 October 2002

**Abstract**

Sediment cover over mid-ocean ridges is expected generally to thicken with seafloor age and distance from spreading center, reflecting symmetric sediment accumulation on both flanks of the ridge. In high quality reflection seismic records and sediment echosounding measurements recently collected across the East Pacific Rise we find a strong asymmetric distribution of sediments. On the eastern flank in the EXCO (Exchange between Crust and Ocean) area at 15°S sediment thickness increases only slowly with distance from the spreading axis, and hence crustal age, to about 15 m on 4.5 Ma old crust and 30 m on 7 Ma old crust. Sediments are draping the basement rather than ponding. On the western flank sediment was sampled that is already 70 m thick on 4.5 Ma old crust and up to 150 m on about 7 Ma old crust. Sediment ponds imply efficient transport by gravitationally driven turbidity currents. Sediment accumulation on the western ridge flanks and the rather flat seafloor indicate a redistribution of sediments. Accumulation of sediments corresponds with the extreme asymmetry of a helium plume at 15°S in the South Pacific. A tongue of high $^{3}$He extending westward from the rise near 2500–2700 m depth and a corresponding tongue of high temperature suggesting that the helium plume introduced by hydrothermal activity on the EPR spreading axis is being carried westward by abyssal currents. Fall-out of hydrothermal plumes may contribute and intensify sedimentation on the western flanks. However, it is reasonable to hypothesize that hydrothermal plumes are important agents in the dispersal of the larvae of hydrothermal vent fauna and may be responsible for the enhancement of pelagic zooplankton biomass resulting in a larger mass of pelagic rain.


*Keywords:* mid-ocean ridge; East Pacific Rise; sediment transport; hydrothermal plume; sedimentation rate

## 1. Introduction

Sediment accumulation on mid-ocean ridges, where distant from terrigenous sources, is pelagic and commonly calcareous ooze. The amount and composition of sediment covering the ridge are controlled by the surface productivity, the crustal age, the carbonate compensation depth (CCD) and the bottom conditions that cause local dissolution and erosion effects. These effects vary geographically and temporally and are complexly interrelated. Variations in pelagic input rates over abyssal hill areas cannot be inferred easily from sedimentation rate variations because sediment thickness fluctuates due to redistribution by

* Corresponding author.
*E-mail address:* hauschild@geophys2.uni-bremen.de (J. Hauschild).

0025-3227/02/$ – see front matter 
PII: S0025-3227(02)00613-8

downslope gravity transport and erosion or non-deposition due to variable fluid shear velocity in the bottom boundary layer of abyssal currents.

In this paper we present a data set from new, high-quality seismic reflection and sediment echosounding measurements. This survey was part of the EXCO (Exchange between Crust and Ocean) project, aimed at studying the impact of off-axis hydrothermalism on the structure and physical properties of oceanic crust (Weigel et al., 1996; Grevemeyer et al., 1999). The EXCO area covers the spreading segment of the East Pacific Rise (EPR) south of the Garrett fracture zone boundary, where the EPR is uncharacteristically devoid of any transform fault boundary for nearly 1150 km (Londsdale, 1989). Here the EPR trends 195° and the tectonic corridor on the Pacific and Nazca Plate intersects the southern EPR near 15°S (Fig. 1). Profiles were surveyed along the seafloor spreading direction to map the thin sedimentary cover on juvenile oceanic crust. Along the EPR the areas of thickest sediment are in the equatorial zone of highest productivity of pelagic organisms. The relatively narrow sediment-free axis of the EPR north of 4°S latitude widens southward of 5°S primarily in response to declining surface productivity (Erlandson et al., 1981). Grevemeyer et al. (1997) investigated the morphology on the eastern flank of the EPR. They documented a positive correlation between increasing relief of abyssal hills and increasing abundance and height of seamounts. Along flowline changes in abyssal hill morphology and seamount size distribution

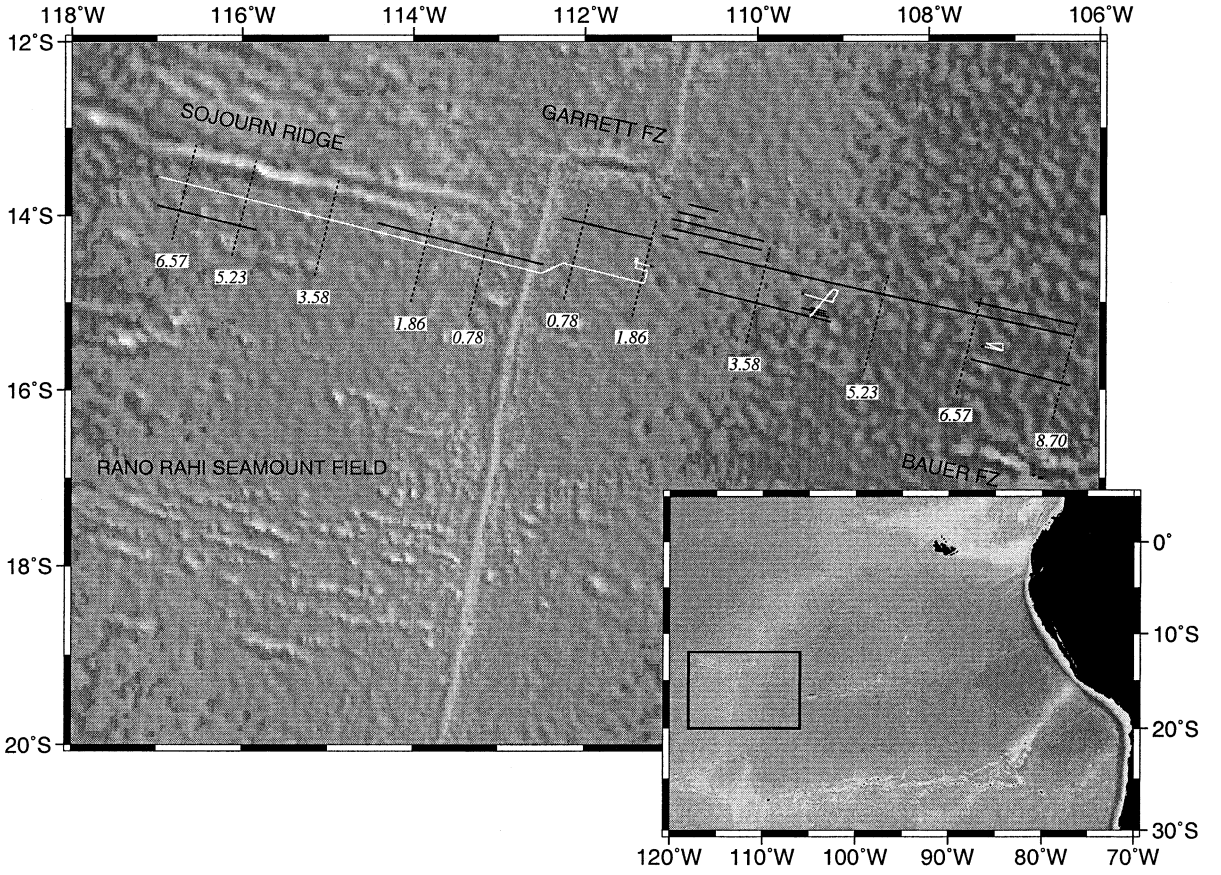


Fig. 1. Location of EXCO II seismic and sediment echosounding surveys across the East Pacific Rise. Bright lines show seismic tracks and black lines show *Parasound* tracks. Dashed lines mark the crustal age (Ma).

correlate with spreading rate changes. Spreading rate changed from 75 m/yr to over 85 m/yr (half rate). South of the Garrett Fracture Zone at 13.5°S spreading is asymmetrical, being faster to the east than to the west. Knowledge of sediment thickness is necessary for the interpretation of heat flow data, because the sedimentary cover inherently affects the hydrogeology in the ridge flanks (Davis et al., 1999). Therefore the knowledge of sedimentation history of the ridge flanks serves different aims. On the western ridge flank profiles are situated between the Sojourn Ridge in the north and a widespread seamount province (Scheirer et al., 1996a,b) in the south. Eastward of the ridge profiles extend to the Bauer Microplate north of the Bauer fracture zone.

## 2. Methods

The EXCO II seismic survey was carried out using a single generator-injector (GI) Gun in 'True GI Mode' with a reduced volume of 1.9 (150 $in^3$) for both the generator and the injector chamber. Along all lines shot spacing was 25 m. Seismic reflection profiles were obtained using a 16-channel 100 m long hydrophone array. Navigation control was derived from global positioning system data in differential mode (DGPS). Locations of seismic lines are shown in Fig. 1. After editing, channels were stacked together to one trace. Processing of profiles consisted of filtering with a bandpass (20–230 Hz) and resampling at 2 ms sampling intervals, deconvolution, and constant velocity w-k-migration. A velocity of 1500 m/s for imaging the thin sediment unit and the top of the basement is sufficient. Because of great water depth and limited aperture of the seismic system, travel-time migration results are not very sensitive to velocity modifications, however, and the quality of the migrated sections is generally very good. Travel times to the seafloor and basement reflections were picked and seafloor and basement depth were interpolated for every trace to obtain sediment thickness. We used a velocity of 1500 m/s to compute sediment thickness. Data processing and picking were done using Seismic Unix (Cohen and Stockwell, 1999). The quality of data allows us to quantify sediment thickness from ridge axis (0.0 Ma old crust) to about 9 Ma old crust with a minimum sediment thickness of about 3 m (Fig. 2). However, in areas of rugged

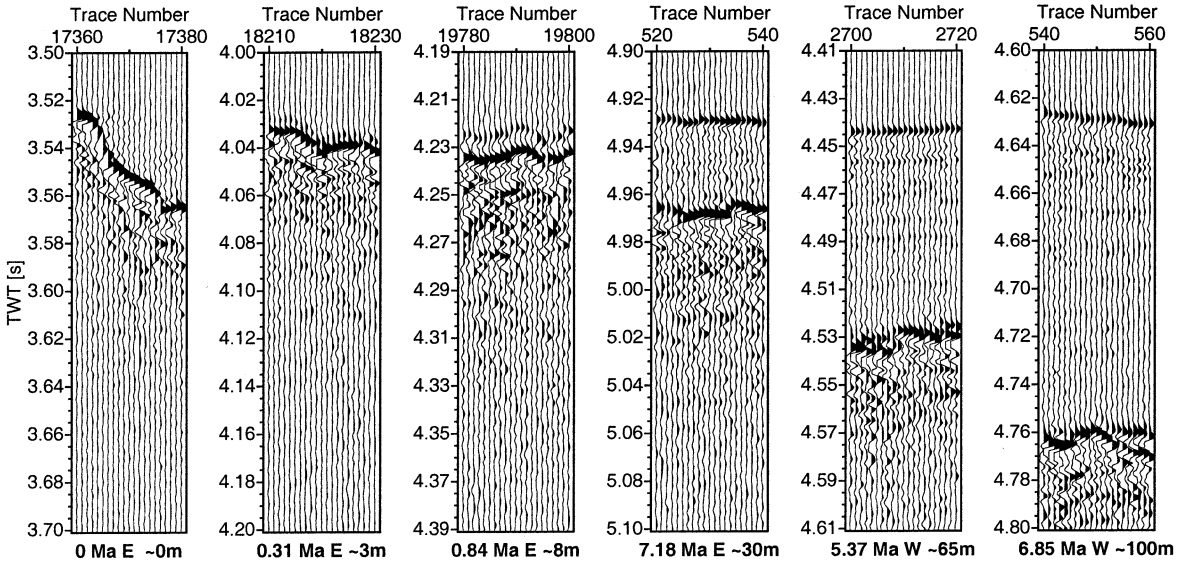


Fig. 2. Seismic panel of sediment thickness across the EPR. Ocean crust with ages from 0 to 7.18 Ma on the western and the eastern ridge flank is shown. Quality of data allows a minimal sediment thickness detection of about 3 m. Thicknesses were derived assuming a 1500 m/s acoustic velocity.

basement relief (i.e. where basement is rough, features are small, or the average slope is steep) with basement arrivals approaching the seafloor, recognition of basement is even more difficult by the strong seafloor reflections. Here sediment thickness smaller than about 10 m is difficult to resolve.

To image the shallow sediment structure down to ~100 mbsf the *Parasound* echosounder is available on RV *SONNE*. The *Paradigma* system (Spiess, 1993) digitizes the data and stores them in SEG-Y format for further processing. Processing of digital *Parasound* records was also done with Seismic Unix. Processing included bandpass filtering (2000–4000 Hz) and a redisplay of envelope amplitudes.

## 3. Results

Seismic sections reveal an asymmetric distribution of sediments. On the eastern flank sediment thickness increases only slowly with distance from the spreading axis, and hence crustal age, to about 15 m on 4.5 Ma old crust (Fig. 3) and 30 m on 7 Ma old crust. Sediments are draping the basement rather than ponding. Draping is confirmed by seismic records (Fig. 4) which reflect the volcanic topography beneath the sediments. Draping implies that sediment has been accumulated from particles locally settled from suspension. On the western flank the structure is quite different. Sediment is already 70 m thick on 4.5 Ma old crust (Fig. 5) and up to 150 m of sediment on about 7 Ma old crust (Fig. 6) was sampled. Horizontally layered sediment ponds imply efficient transport and resedimentation by turbidity currents. The East Pacific Rise acts as a distinct barrier for the style of sedimentation between the west flank, where ponding is evident, and the east flank, where no ponding occurs.

Comparison of *Parasound* and seismic data shows how they complement one another. The sediment echosounder (Fig. 7a) displays the individual sediment layers of the uppermost units down to max. 40 m depth. Seismic section (Fig. 6) shows the whole 150 m of sediment unit covering volcanic bedrock. Eastward of the spreading center the interpretation of *Parasound* sections is more difficult. A pattern of overlapping hyperbolas (Fig. 7b,c) is caused by the fine scale topography. Knowledge of sediment thickness from seismic data in these regions allows a classification of sediment thickness from *Parasound* data. Thus

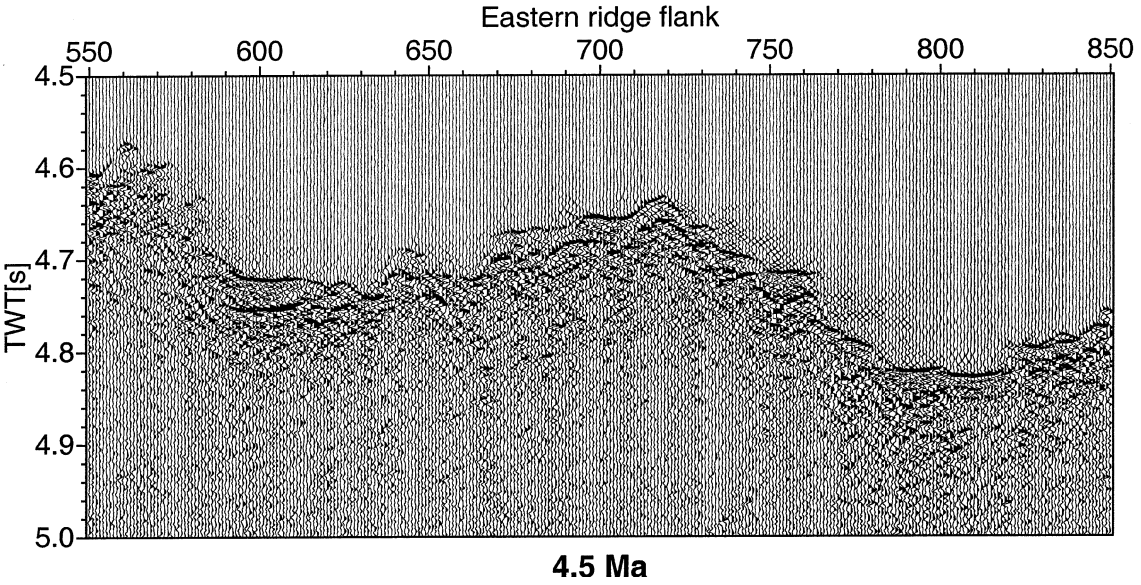


Fig. 3. Seismic section of 4.5 Ma old crust on the eastern ridge flank.

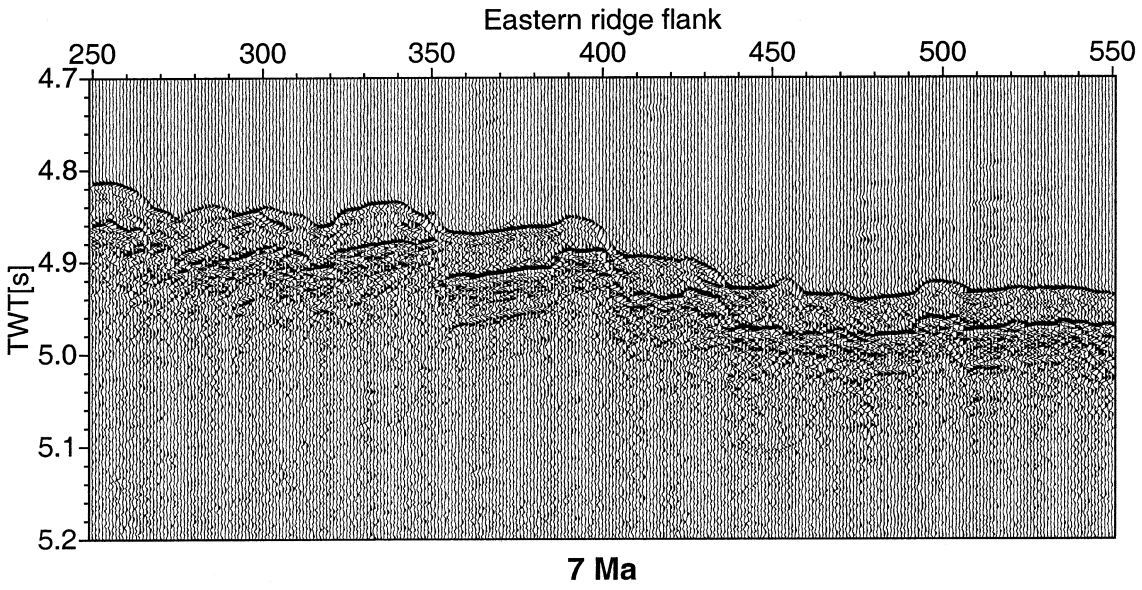


Fig. 4. Seismic section of 7 Ma old crust on the eastern ridge flank.

sediment thickness on 1.1 Ma old crust (Fig. 7b) is 10 m and on 7 Ma old crust (Fig. 7c) it is about 30 m. A sediment unit of 20–25 m thickness buries the 8.7 Ma old crust on the easternmost part of the corridor (Fig. 7d). The sediment thickness values from *Parasound* are used to close the gap between seismic profiles on the eastern ridge flank.

Sediment thickness increases more or less continuously from the ridge axis towards the west. The data suggest that the average sedimentation rate for the west flank of the 15°S East Pacific

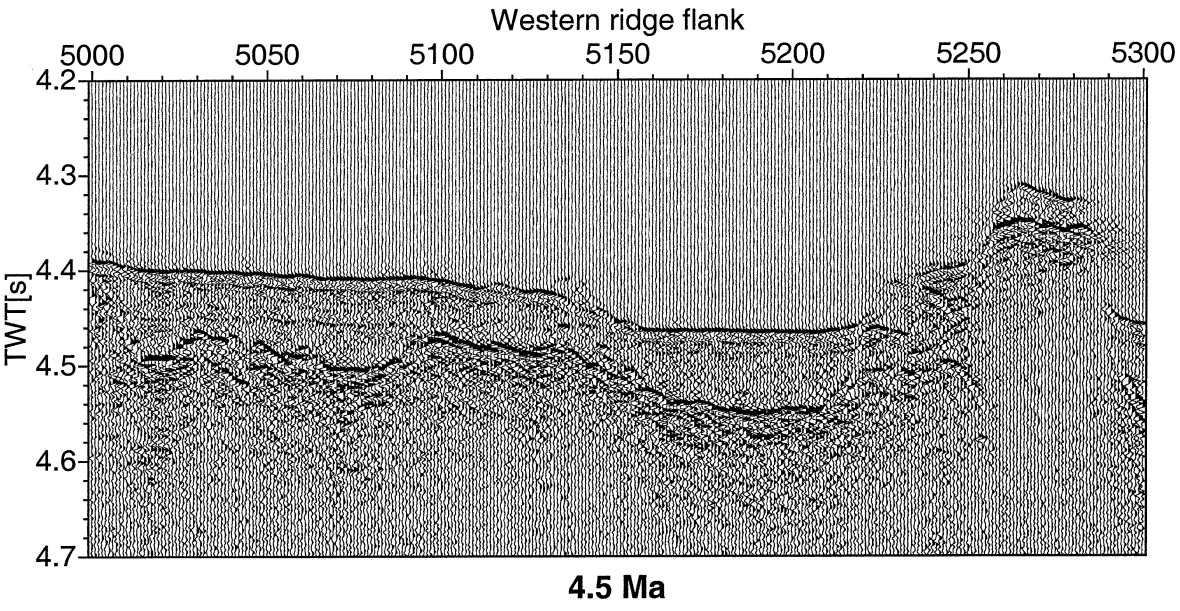


Fig. 5. Seismic section of 4.5 Ma old crust on the western ridge flank.

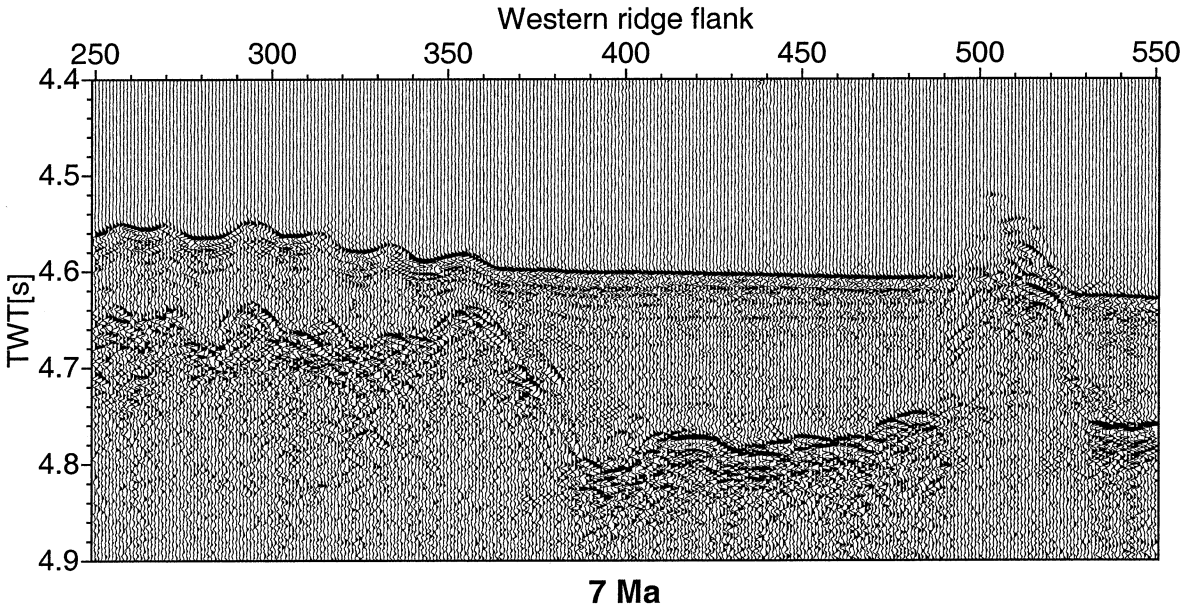


Fig. 6. Seismic section of 7 Ma old crust on the western ridge flank.

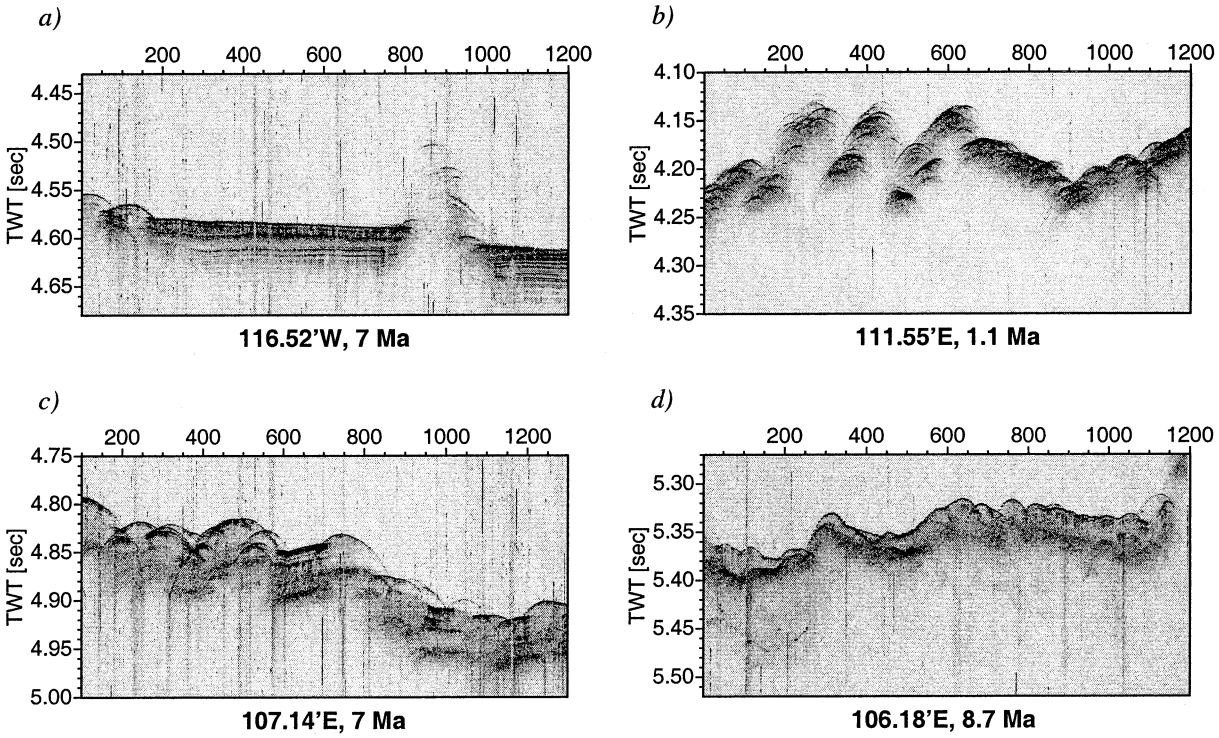


Fig. 7. *Parasound* sections showing sediment units on the flanks of the EPR. (a) Western ridge flank, 7 Ma old crust. (b) Eastern ridge flank, 1.1 Ma old crust. (c) Eastern ridge flank, 7 Ma old crust. (d) Eastern ridge flank, 8.7 Ma old crust.

Rise area has been about 10 m/Myr for the last 7 Ma (Fig. 8). The lack of sediments at 3.5, 4 and 5 Ma correlates with large seamounts in this region. Sediment on the steep seamount flanks is forced downhill to be accumulated in the adjacent grabens. On the eastern flank, the graph of sediment thickness fits the model line of systematic thickness variation expected for 10 m/Ma only for the first 2 Ma. On crust older than 2 Ma the sediment thickness increases only slowly from 20 m to about 30 m on about 9 Ma crust, which corresponds to a sedimentation rate of less than 2 m/Ma in this period. The increase of the sedimentation rate on both flanks for the first 2 Ma is nearly the same and from this time the accumulation of sediment on the flanks varies by an order of magnitude.

Seafloor picks show the bathymetry of the western and eastern ridge flank along the seismic lines (Fig. 8). The axis of the EPR is a blocky ridge about 300 m high and 10 km wide without a central valley, but a median high. The shallowest depth of the ridge is 2600 m. Away from the ridge axis, the topography of the western flank is characterized by abyssal hills 5–15 km wide and 200–300 m in relief. On crust between 3 and 5 Ma old, seamounts with a height of 500–1000 m occur.

The topography of the eastern flank shows abyssal hills and the intervening valleys in a smaller dimension than on the western flank. Eastward

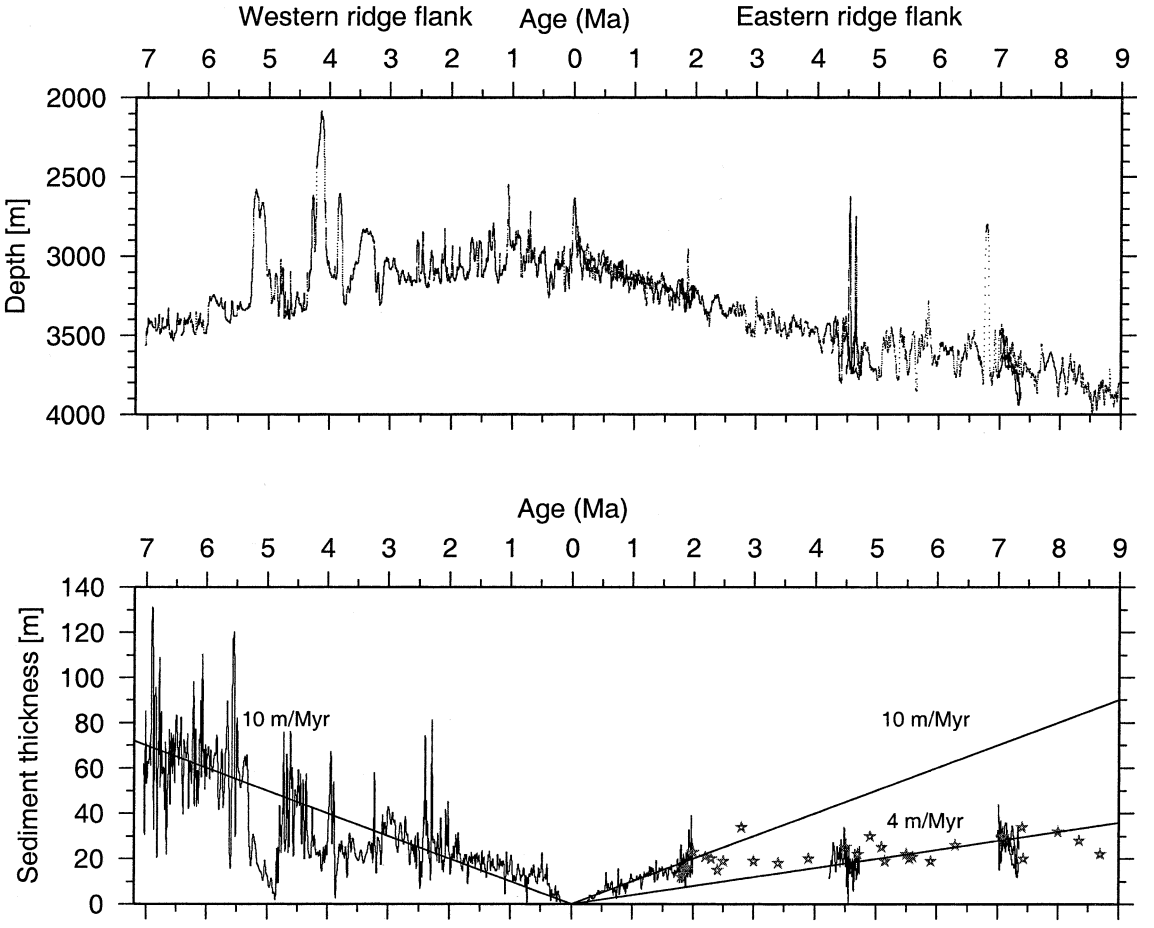


Fig. 8. Topography and sediment thickness plotted versus crustal age measured along the seafloor spreading direction. Thicknesses were derived assuming a 1500 m/s acoustic velocity. The oblique lines show the sediment thickness variation expected for constant sedimentation. Stars give thickness from *Parasound*.

of the ridge, on up to 2 Ma old crust, the hills are about 5 km wide and 100–150 m in relief. The seafloor subsides asymmetrically from ridge axis to 7 Ma old crust to a depth of 3400–3500 m in the west and to a depth of 3700–3900 m in the east.

## 4. Discussion

In addition to local basement and sedimentary structures, the seismic data presented in this paper provide constraints on regional basement topography and sediment thickness variations.

Sediment distribution across the EPR shows a consistent asymmetry, with sediment about three times as thick on the western flank as on the eastern flank.

Where bottom currents are weak or the pelagic supply rate is high, the sediments are generally expected to thicken systematically with seafloor age and distance from spreading centers, reflecting progressive accumulation such as the intermediate spreading Galapagos spreading center (Mitchell, 1995, 1998). Moreover, sediment thickness may show deviations from the obvious sediment trends that are governed by productivity of surface water, ocean currents, hydrothermal activity, and water depth. Symmetric sediment accumulation can be modified by variable carbonate dissolution with depth and time, which can sometimes reverse the thickening trend.

Along the equator the largest sediment thickness is found due to the high productivity of surface water. It decreases generally in both directions toward the north and the south (Laske and Masters, 1997). The profiles on both flanks of the EPR should show a similar sediment distribution (Ewing and Ewing, 1967), since the transect is oriented approximately east–west parallel to the equator. In contrast, in the area of the EPR, a clear west–east deviation in sediment thickness is observed. Here a difference in the productivity of the surface water was not expected.

Comparison of western and eastern ridge topography shows that the subsidence trend for the western flank is much lower. Anderson and Sclater (1972) already noted asymmetry in bathymetric profiles across the rise. This feature was also described in previous studies (e.g. Cochran, 1986) and might be due to some unusual lithospheric and/or asthenospheric properties beneath the Pacific plate (Scheirer et al., 1996a,b; Grevemeyer et al., 1997). The distinct asymmetric subsidence of ridge flanks could provide one explanation for the different sediment thicknesses. Thus, with faster increasing depth on the eastern flank, the carbonates could be dissolved more rapidly and so lead to a decrease of the deposit. The CCD and the lysocline in the equatorial eastern Pacific were determined by Berger et al. (1976) to be about 4000 m and about 3500 m, respectively. Though topography indicates asymmetric subsidence with higher rates towards the east, water depth is always above CCD. The 3500 m top of the transition zone intersects the bathymetry at around 4 Ma, whereas the change in sediment thickness trend starts at 2 Ma. During the second leg of cruise SO145 gravity cores were studied for acquiring the sediment composition. They show calcareous micrite with coccolithic material of 80–90% in sediment samples on up to 9 Ma old crust on the eastern flank (C. Devey and K. Lackschewitz, personal communication). This rules out any dissolution of carbonate. Moreover, a sediment thickness of 110 m in Bauer Deep (DSDP Site 319, Shipboard Scientific Party, 1976) in a water depth of 4300 m does not agree with a carbonate compensation origin.

Erlandson et al. (1981) attributed the asymmetrical sediment accumulation on the flanks of the EPR in part to asymmetric spreading. Using magnetic anomalies from Cormir et al. (1996), it appears that up to anomaly 3 seafloor spreading towards the east was around 86 mm/yr, while it was only 68 mm/yr towards the west. But this non-uniform seafloor spreading does not explain the pronounced asymmetrical sediment distribution with respect to seafloor age, nor the asymmetry in bathymetry(Fig. 8).

Sediment accumulation on the western ridge and the rather flat sediment surface indicate a redistribution of sediments. Sediment thickness may generally fluctuate by downslope gravity transport and deposition rate variability or erosion due to

variable fluid shear velocity in the bottom boundary layer of abyssal currents. While at the slow-spreading Mid-Atlantic Ridge the topographic roughness is larger than on the fast-spreading EPR (Malinverno, 1991) and turbidity currents initiated by sediment slides occur (Mitchell et al., 1998), the seafloor relief at the fast-spreading East Pacific Rise is relatively subdued. The influence of the Sojourn Ridge to the north could contribute as a source for turbidites, resulting in thicker sediment units on the western flank but not of this great dimension. In general there is more sediment on the western flank along this ridge segment. To the south, side-scan data confirm greater sediment thickness on the western flank than on the eastern flank in the MELT area (M. Cormier, personal communication). Thus, bottom currents are probably the main cause of asymmetric distribution of sediments. In the South Pacific between 10°S and 20°S a westward flow prevails from the sea surface to 4000 m depth (Reid, 1986). Consequently, distribution of sediment is governed by lateral transport by bottom currents.

However, a current directed westward cannot alone cause the observed pattern of sediment distribution. With a constant but latitude-dependent formation of pelagic sediment, a westward current should lead to uniformly distributed deposit on the eastern side as well. Since the EPR even acts as a distinct barrier, it should generate a larger deposit of sediment on the eastern side rather than on the western flank of the EPR. The asymmetrical distribution of sediments across the EPR at 15°S can be explained conclusively with a westward current if the sediments are generated at the EPR and their production is triggered at the EPR, respectively.

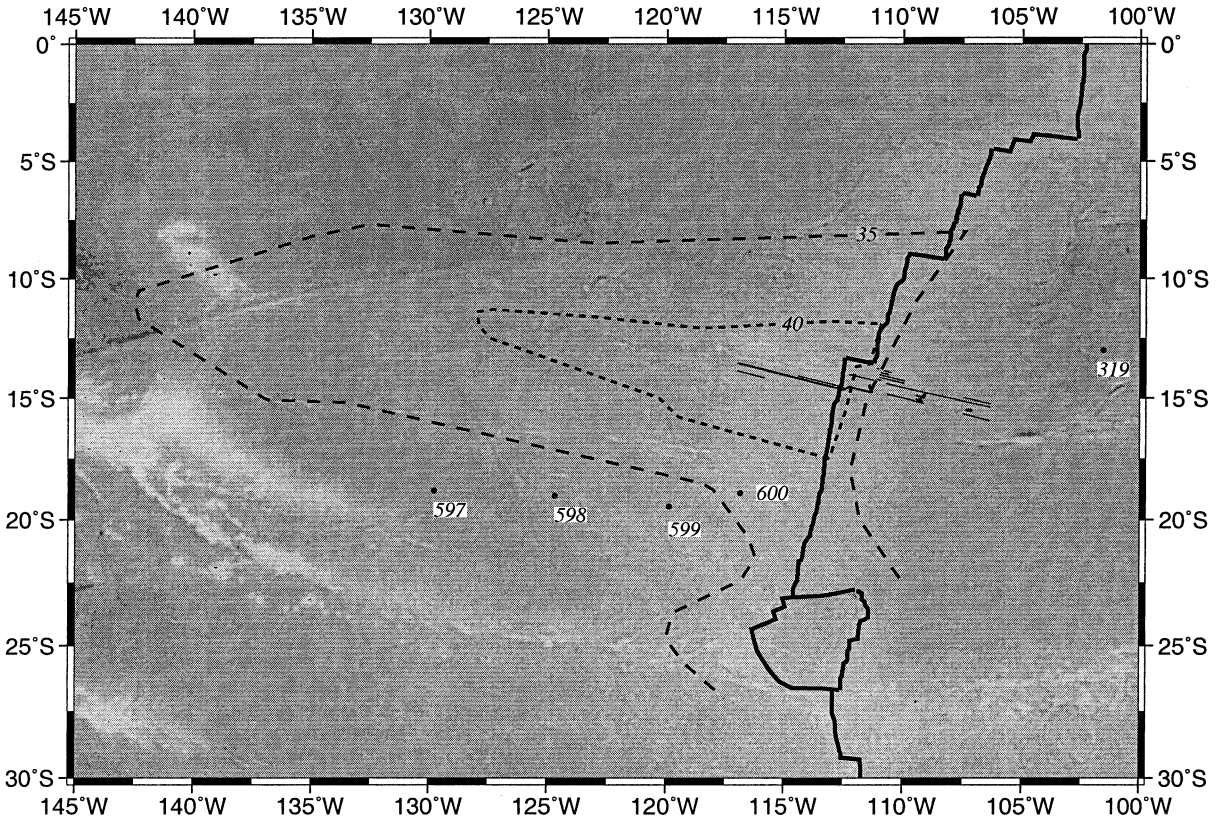


Fig. 9. Shape of hydrothermal plume marked by $^{3}He$ distribution from Lupton (1995). Contour lines of $^{3}He/^{4}He$ ratios in units of $\delta(^{3}He)\%$ are broken. Thin lines show seismic and sediment echosounding surveys. Dots are DSDP drill sites.

Plumes are an important mechanism of dispersal for the thermal and chemical fluxes introduced at seafloor hotsprings. Although the details are poorly understood, it is likely that plumes are also important agents in the dispersal of the larvae of hydrothermal vent fauna and may be responsible for the enhancement of pelagic zooplankton biomass. The true expanse of hydrothermal plumes in the deep ocean was published by Lupton and Craig (1981). Their $^3$He section spans the EPR at 15°S (Fig. 9). This section showed an asymmetric helium plume extending over 2000 km to the west of the EPR crest, but having almost no expression to the east of the ridge axis. The helium plume in the south Pacific is still one of the best examples of a far field plume (Lupton, 1995). The extreme asymmetry of this plume suggests that the $^3$He introduced by hydrothermal activity on the EPR spreading axis is being carried westward by abyssal currents. The plume takes the form of an elongated jet trending slightly WNW, in general agreement with the shape of Reid's (1982) thermal plume. The east–west asymmetry is well pronounced. These mid-depth water currents also disperse the fine-grained particulates derived from hydrothermal venting until they eventually settle out to form metal-enriched sediments beneath the overlying plume (Mills and Elderfield, 1995), resulting in a greater deposition rate of hydrothermal material on the western flank of the EPR than on the eastern flank (Marchig et al., 1986). Actively forming hydrothermal mineral deposits provide a source of energy for chemosynthesis and a substratum for colonization by adult and larval vent organisms. Since mineral deposition and organism growth can occur within similar time frames, their potential for interactions is substantial (Juniper and Sarrazin, 1995). At latitude 15°S the $^3$He signal decreases to the regional backround values at a short distance to the east of the EPR crest. This observation corresponds with the small region of higher sedimentation rate near the EPR and the lower sedimentation rate on crust older than 2 Ma on the eastern flank. On the western flank the sediment echosounding survey is located in the center of the hydrothermal plume, representing the highest values of $^3$He. The extension of $^3$He-rich water over 2000 km to the west at 15°S decreases to about 300 km at 20°S. Here the east–west asymmetry turns into a symmetric expanse of the hydrothermal plume. Sediment thicknesses at DSDP Sites 597–600 (Shipboard Scientific Party, 1986) near 20°S (Fig. 9) show an accumulation similar to the east flank at 15°S, with a sediment thickness of 21 m on 5 Ma old crust, 41 m on 8.5 Ma old crust, and about 53 m on 17 and 29 Ma old crust on the western flank. The band of a westward ocean current in the area of investigation may be affected by large topographic reliefs like the Sojourn Ridge on the Pacific plate near 13°S and the Rano Rahi seamount field between 17°S and 19°S (Scheirer et al., 1996a,b), increasing somehow the sediment accumulation on the western ridge flank.

## Acknowledgements

We are grateful to N.C. Mitchell and an anonymous referee for helpful remarks and suggestions. We thank the captain, officers and crew of the R/V *SONNE* (leg 145-1) for their support at sea. This work was funded by the German Federal Ministery of Education, Science, Research and Technology (Grant 03G0145A).

## References

Anderson, R.N., Sclater, J.G., 1972. Topography and evolution of the East Pacific Rise between 5°S and 20°S. Earth Planet. Sci. Lett. 14, 433–441.

Berger, W.H., Adelseck, C.G., Mayer, L.A., 1976. Distribution of carbonate in surface sediments of the Pacific Ocean. J. Geophys. Res. 81 (15), 2617–2627.

Cohen, J.K., Stockwell, J.K., Jr., 1999. CWP/SU: Seismic Unix Release 33: a free package for seismic research and processing. Center for Wave Phenomena, Colorado School of Mines.

Cochran, J.R., 1986. Variations in subsidence rate along intermediate and fast spreading mid-ocean ridges. Geophys. J. R. Astron. Soc. 87, 421–454.

Cormir, M.-H., Scheirer, D.S., Macdonald, K.C., 1996. Evolution of the East Pacific Rise at 16°-19° since 5 Ma: bisection of overlapping spreading centers by new, rapidly propagating segments. Mar. Geophys. Res. 18, 53–84.

Davis, E.E., Chapman, D.S., Wang, K., Villinger, H., Fisher, A.T., Robinson, S.W., Grigel, J., Probonow, D., Stein, J.,

Becker, K., 1999. Regional heat flow variations across the sedimented Juan de Fuca Ridge eastern flank: Constraints on lithospheric cooling and lateral hydrothermal heat transport. J. Geophys. Res. 104, 17675–17688.

Erlandson, D.L., Hussong, D.M., Campell, J.F., 1981. Sediment and associated structure of the northern Nazca plate. Geol. Soc. Am. Mem. 154, 295–314.

Ewing, J.I., Ewing, M., 1967. Sediment distribution on the mid-ocean ridges with respect to spreading of the sea floor. Science 156, 1590–1592.

Grevemeyer, I., Renard, V., Jennrich, C., Weigel, W., 1997. Seamount abundances and abyssal hill morphology on the eastern flank of the East Pacific Rise at 14 degrees S. Geophys. Res. Lett. 24, 1955–1958.

Grevemeyer, I., Kaul, N., Villinger, H., Weigel, W., 1999. Hydrothermal activity and the evolution of the seismic properties of upper oceanic crust. J. Geophys. Res. 104, 5069–5079.

Juniper, S.K., Sarrazin, J., 1995. Interaction of Vent Biota and Hydrothermal Deposits: Present Evidence and Future Experimentation. Geophys. Monogr. Ser. 91, 178–193.

Laske, G., Masters, G., 1997. A global digital map of sediment thickness. EOS Trans. AGU 78, F483.

Londsdale, P., 1989. Segmentation of the Pacific-Nazca spreading center, 1°N-20°S. J. Geophys. Res. 94, 12197–12225.

Lupton, J.E., Craig, H., 1981. A major $^{3}$He source on the East Pacific Rise. Science 214, 13–18.

Lupton, J.E., 1995. Hydrothermal plumes: near and far field. Geophys. Monogr. Ser. 91, 317–346.

Malinverno, A., 1991. Inverse square-root dependence of mid-ocean-ridge flank roughness on spreading rate. Nature 352, 58–60.

Marchig, V., Erzinger, J., Heinze, P.-M., 1986. Sediment in the black smoker area of the East Pacific Rise (18.5°S). Earth Planet. Sci. Lett. 79, 93–106.

Mills, R.A., Elderfield, H., 1995. Hydrothermal activity and the geochemistry of metalliferous sediment. Geophys. Monogr. Ser. 91, 392–407.

Mitchell, N.C., 1995. Chracterising the extent of volcanism at the Galapagos Spreading Centre using Deep Tow sediment profiler records. Earth Planet. Sci. Lett. 134, 459–472.

Mitchell, N.C., 1998. Sediment accumulation rates from Deep Tow profiler records and DSDP Leg 70 cores over the Galapagos spreading centre. In: Cramp, A., MacLeod, C.J., Lee, S.V., Jones, E.J.W. (Eds), Geological Evolution of Ocean Basins: Results from the Ocean Drilling Program. Geol. Soc. London Spec. Publ. 131, pp. 199–209.

Mitchell, N.C., Allerton, S., Escartin, J., 1998. Sedimentation on young ocean floor at the Mid-Atlantic Ridge, 29°S. Mar. Geol. 148, 1–8.

Reid, J.R., 1982. Evidence on an effect of heat flux from the East Pacific Rise upon the characteristics of mid-depth waters. Geophys. Res. Lett. 9, 381.

Reid, J.R., 1986. On the geostrophic circulation of the South pacific Ocean: Flow patterns, tracers and transport. Prog. Oceanogr. 16 (1), 149–244.

Scheirer, D.S., Macdonald, K.C., Forsyth, D.W., Miller, S.P., Wright, D.J., Cormier, M.-H., Weiland, C.M., 1996a. A map series of the Southern East Pacific Rise and its flanks, 15 degrees S to 19 degrees S. Mar. Geophys. Res. 18, 1–12.

Scheirer, D.S., Macdonald, K.C., Forsyth, D.W., Miller, S.P., Wright, D.J., Cormier, M.-H., Weiland, C.M., 1996b. Abundant seamounts of the Rano Rahi Seamount Field near the Southern East Pacific Rise, 15 degrees S to 19 degrees S. Mar. Geophys. Res. 18, 13–52.

Shipboard Scientific Party, 1986. DSDP Leg 92, Site 597-600. In: Leinen, M., Rea, D.K., et al. (Eds.), Init. Repts. DSDP 92, U.S. Govt. Print. Off., Washington, DC.

Shipboard Scientific Party, 1976. DSDP Leg 34, Site 319. In: Yeats, R.S., Hart, S.R., et al. (Eds.), Init. Repts. DSDP, 34, U.S. Govt. Print. Off., Washington, DC.

Spiess, V., 1993. Digitale Sedimentechographie - Neue Wege zu einer hochauflösenden Akustostratigraphie. Berichte aus dem Fachbereich Geowissenschaften der Universität Bremen, Universität Bremen, 35, 199 pp.

Weigel, W., Grevemeyer, I., Kaul, N., Villinger, H., Lüdmann, T., Wong, H.K., 1996. Aging of oceanic crust at the southern east Pacific Rise. EOS, Trans. Am. Geophys. Union 77, 504.